Laboratory of Economics and Management

Sant'Anna School of Advanced Studies
Piazza Martiri della Libertà, 33 - 56127 PISA (Italy)
Tel. +39-050-883-343 Fax +39-050-883-344
Email: lem@sssup.it Web Page: http://www.lem.sssup.it/

# LEM

## Working Paper Series

# Rewiring World Trade. Part II: A Weighted Network Analysis

Tiziano Squartini *
Giorgio Fagiolo °
Diego Garlaschelli §

* Department of Physics, University of Siena, Italy
° LEM-Scuola Superiore Sant'Anna, Pisa, Italy
§ LEM-Scuola Superiore Sant'Anna, Pisa, Italy, and Leiden Institute of Physics, Leiden, NL

2011/09 March 2011

ISSN (online) 2284-0400

# Rewiring World Trade. Part II: A Weighted Network Analysis

Tiziano Squartini
*CSC and Department of Physics, University of Siena, Via Roma 56, 53100 Siena (Italy)*

Giorgio Fagiolo
*LEM, Sant'Anna School of Advanced Studies, 56127 Pisa (Italy)*

Diego Garlaschelli
*LEM, Sant'Anna School of Advanced Studies, 56127 Pisa (Italy) and*
*Instituut-Lorentz for Theoretical Physics, Leiden Institute of Physics,*
*University of Leiden, Niels Bohrweg 2, 2333 CA Leiden (The Netherlands)*
(Dated: March 7, 2011)

In this sequel to a companion paper, we complement our analysis of the binary projections of the International Trade Network (ITN) by considering its weighted representations. We show that, unlike the binary case, all possible weighted representations of the ITN (directed/undirected, aggregated/disaggregated) cannot be traced back to local structural properties, which are therefore of limited informativeness. Our results highlight that any topological property representing only partial information (e.g., degree sequences) cannot in general be obtained from the corresponding weighted property (e.g., strength sequences). Therefore the expectation that weighted structural properties offer a more complete description than purely topological ones is misleading. Our analysis of the ITN detects indirect effects that are not captured by traditional macroeconomic analyses focused only on weighted first-order country-specific properties, and highlights the limitations of models and theories that overemphasize the need to reproduce and explain such properties.

PACS numbers: 89.65.Gh; 89.70.Cf; 89.75.-k; 02.70.Rr

## I. INTRODUCTION

In this paper we extend our analysis of the binary projection of the International Trade Network (ITN) reported in the previous paper [1] to the weighted representation of the same network. As in the binary case, we employ a recently-proposed randomization method [2] to assess in detail the role that local properties have in shaping higher-order patterns of the weighted ITN in all its possible representations (directed/undirected, aggregated/disaggregated) and across several years. We find that, unlike the binary case, higher-order patterns of weighted (either directed or undirected, either aggregated or disaggregated) representations of the ITN cannot be merely traced back to local properties alone (i.e., node strength sequences). In particular, when compared to its randomized variants, the observed weighted ITN displays a different and sparser topology (despite the ITN is usually considered denser than most studied networks), stronger disassortativity, and larger clustering. As sparser and less aggregated commodity-specific representations are considered, the accordance between the real and randomized networks gets even worse. All these results hold for both undirected and directed projections, and are robust throughout the time interval we consider (from year 1992 to 2002).

From an international-trade perspective, our results indicate that a weighted network description of trade flows, by focusing on higher-order properties in addition to local ones, captures novel and fresh evidence. Therefore, traditional analyses of country trade profiles focusing only on local properties and country-specific statistics convey a partial description of the richness and details of the ITN architecture. Moreover, economic models and theories that only aim at explaining the local properties of the weighted ITN (i.e. the total values of imports and exports of world countries) are limited, as such properties have no predictive power on the rest of the structure of the network.

We refer the reader to the companion paper [1] for a description of the data, the notation used, the meaning and economic importance of local topological properties, and the randomization method that we have adopted.

## II. THE ITN AS A WEIGHTED UNDIRECTED NETWORK

The weighted representation of the ITN takes into account the intensity (dollar value) of trade relationships, and can be either directed or undirected. The structure of the network is completely specified by the weight matrix $\mathbf{W}$, whose entries $\{w_{ij}\}$ have been defined in Ref. [1] in the directed and undirected case. In both cases, we first use the matrix $\mathbf{W}$ as the starting point for the randomization method, and as a result we obtain an ensemble of randomized weight matrices with fixed local constraints (the strength sequences). Then, we rescale both the real matrix and its randomized counterparts by dividing all weights by the total yearly weight $w_{tot} = \sum_{ij} w_{ij}$. Note that $w_{tot}$ is the sum of the strengths of all vertices, and is therefore preserved by the method in all randomized networks, as a result of the constraints on the strengths. This procedure allows for homogeneous comparisons between real and randomized webs, and across different years and commodities.

In the weighted undirected case, an edge between vertices $i$ and $j$ represents the presence of at least one of the two possible trade relationships between the two countries $i$ and $j$, and the weight $w_{ij}$ represents the average trade value (or equivalently half the total bilateral trade value) [1]. Clearly, if no trade occurs in either direction, then $w_{ij} = 0$ and no link exists. The weight matrix $\mathbf{W}$ is therefore symmetric: $w_{ij} = w_{ji}$. One can still define an adjacency matrix $\mathbf{A}$, describing the purely binary topology of the network, with entries $a_{ij} = \Theta(w_{ij})$ where $\Theta(x) = 1$ if $x > 0$ and $\Theta(x) = 0$ otherwise. Clearly, the symmetry of $\mathbf{W}$ implies the symmetry of $\mathbf{A}$. In the weighted undirected representation the local constraints $\{C_a\}$ are the strengths of all vertices, i.e. the *strength sequence* $\{s_i\}$ [1]. The randomization method [2] proceeds in this case by specifying the constraints $\{C_a\} \equiv \{s_i\}$ (see Appendix A), and yields the ensemble probability of any weighted graph $\mathbf{G}$, which now is uniquely specified by its generic weight matrix $\mathbf{W}$. For any weighted topological property $X$, it is therefore possible to easily obtain the expectation value $\langle X \rangle$ across the ensemble of weighted undirected graphs with specified strength sequence. In economic terms, specifying the strength sequence amounts to investigate the properties of the trade network once total trade of all countries is controlled for. By construction, the expected strength $\langle s_i \rangle$ across the randomized ensemble is equal to the empirical value $s_i$, therefore in the weighted undirected case the strength values $\{s_i\}$ are the natural independent variables in terms of which other weighted properties $X$ can be visualized. However, as we mentioned in the companion paper [1], in order to allow a consistent temporal analysis we need to use the rescaled weights $\tilde{w}_{ij} \equiv w_{ij}/w_{tot}$. Consistently, we define the rescaled strength

$$\tilde{s}_i \equiv \sum_{j \neq i} \tilde{w}_{ij} = \frac{s_i}{w_{tot}} \tag{1}$$

(where $w_{tot} = \sum_i \sum_{j<i} w_{ij}$) and we similarly use $\tilde{w}_{ij}$ instead of $w_{ij}$ in the definition of all other weighted topological quantities. Note that, across the randomized ensemble, $w_{tot}$ is a random variable, since so are the weights $w_{ij}$. However, we can rewrite $w_{tot} = \sum_i s_i/2$, and since $\langle s_i \rangle = s_i$ we have

$$\langle w_{tot} \rangle = \frac{\sum_i \langle s_i \rangle}{2} = \frac{\sum_i s_i}{2} = w_{tot} \tag{2}$$

The above result shows that the expectation value of the total weight across the randomized ensemble is constrained by the method to be strictly equal to the observed value $w_{tot}$. In other words, the constraint on the strengths is automatically reflected also in a constraint on the total weight, and we can therefore use the the latter to rescale all weights, both in the real network and in its randomized variants.

As for the binary analyses [1], we first report detailed results for the 2002 snapshot of the commodity-aggregated network (Sections II A and II B) then consider the temporal evolution of the aggregated network (Sections II C and II D), and finally perform a commodity-specific analysis (Section II E).

### A. Average nearest neighbor strength

We start with the analysis of the completely aggregated network (i.e. $c = 0$ according to our notation described in Ref. [1]). Therefore, in the following formulas, we set $\mathbf{W} \equiv \mathbf{W}^0$ and drop the superscript for brevity. Our aim is to understand how specifying the strength sequence affects higher-order properties. We start with the weighted counterpart of the average nearest neighbor degree (ANND), i.e. the *average nearest neighbor strength* (ANNS) of vertex $i$, defined as

$$\tilde{s}_i^{nn} \equiv \frac{\sum_{j \neq i} a_{ij} \tilde{s}_j}{k_i} = \frac{\sum_{j \neq i} \sum_{k \neq j} a_{ij} \tilde{w}_{jk}}{\sum_{j \neq i} a_{ij}} \tag{3}$$

The ANNS measures the average strength of the neighbors of a given vertex. Similarly to the ANND, the ANNS involves indirect interactions of length 2, however (as happens for most weighted quantities) mixing both weighted and purely topological information: in particular, terms of the type $a_{ij}\tilde{w}_{jk}$ appear in the definition. The correlations between the strength of neighboring countries can be inspected by plotting $\tilde{s}_i^{nn}$ versus $\tilde{s}_i$. This is shown in Fig. 1. Even if the points are now significantly more scattered, we find a decreasing trend as previously observed for the corresponding binary quantities [1]. This trend signals that highly trading countries trade typically with poorly trading ones (and vice versa), confirming on a weighted basis the disassortative character observed at the binary level. However, in this case the null model behaves in a completely different way: over the randomized ensemble with specified strength sequence, the expectation value $\langle \tilde{s}_i^{nn} \rangle$ of the ANNS (see Appendix A) decreases over a much narrower range (see Fig. 1), and is always different from the observed value. This important results implies that, even if we observe disassortativity in both cases (binary and weighted), we find that in the binary case this property is completely explained by the degree sequence, whereas in the weighted case it is not explained by the strength sequence. This has implications for economic models of international trade: while no theoretical explanation is required in order to explain why poorly connected countries trade with highly connected ones on a binary basis (once the number of trade partners is specified), additional explanations are required in order to explain the same phenomenon at a weighted level, even after controlling for the total trade volumes of all countries. This result could look counterintuitive, as a simple visual inspection would suggest that in the binary case the disassortative behavior is in absolute terms

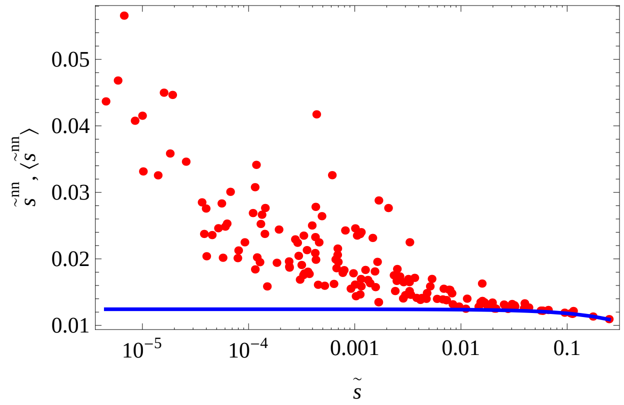


FIG. 1: Average nearest neighbor strength $\tilde{s}_i^{nn}$ versus strength $\tilde{s}_i$ in the 2002 snapshot of the real weighted undirected ITN (red points), and corresponding average over the maximum-entropy ensemble with specified strengths (blue curve).

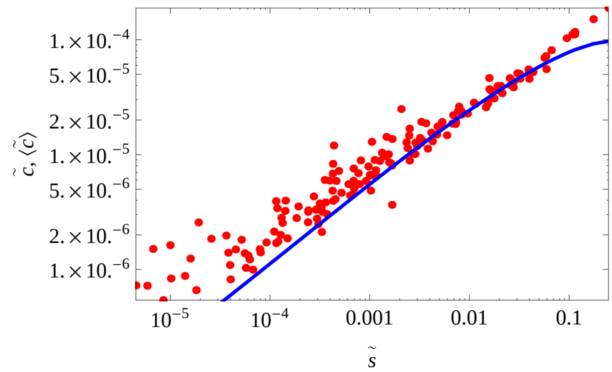


FIG. 2: Weighted clustering coefficient $\tilde{c}_i$ versus strength $\tilde{s}_i$ in the 2002 snapshot of the real weighted undirected ITN (red points), and corresponding average over the maximum-entropy ensemble with specified strengths (blue curve).

less noisy, and sometimes more pronounced, than in the weighted one.

### B. Weighted clustering coefficient

We now consider the weighted version of the clustering coefficient. In particular, we choose the definition proposed in Ref. [3], which has a more direct extension to the directed case [4]. According to that definition, the (rescaled) *weighted clustering coefficient* $\tilde{c}_i$ represents the intensity of the triangles in which vertex $i$ participates:

$$\begin{aligned}\tilde{c}_i &\equiv \frac{\sum_{j\neq i}\sum_{k\neq i,j}(\tilde{w}_{ij}\tilde{w}_{jk}\tilde{w}_{ki})^{1/3}}{k_i(k_i-1)} \\ &= \frac{\sum_{j\neq i}\sum_{k\neq i,j}(\tilde{w}_{ij}\tilde{w}_{jk}\tilde{w}_{ki})^{1/3}}{\sum_{j\neq i}\sum_{k\neq i,j}a_{ij}a_{ik}}\end{aligned} \qquad (4)$$

Note that $\tilde{c}_i$ takes into account indirect interactions of length 3, corresponding to products of the type $\tilde{w}_{ij}\tilde{w}_{jk}\tilde{w}_{ki}$ appearing in the above formula. In Fig. 2 we plot $\tilde{c}_i$ versus $\tilde{s}_i$. This time we find an increasing trend of $\tilde{c}_i$ as a function of $\tilde{s}_i$, indicating that countries with larger total trade participate in more intense trade triangles. We also show the trend followed by the randomized quantity $\langle\tilde{c}_i\rangle$ (see Appendix A), which is found to approximately reproduce the empirical data. Despite the partial accordance between the clustering profile of real and randomized networks, the total level of clustering of the real ITN is however larger than its randomized counterpart, as we show below (Section II C) for all the years considered.

### C. Evolution of weighted undirected properties

The results we have reported above are qualitatively similar for each of the 11 shapshots of the ITN from year 1992 to 2002. As for our binary analyses [1], we can therefore compactly describe the temporal evolution of weighted undirected properties in terms of simple indicators.

We start with the analysis of the ANNS (Fig. 3). In Fig. 3a we report the average (across vertices) and the associated 95% confidence interval of both real and randomized values ($\{\tilde{s}_i^{nn}\}$ and $\{\langle\tilde{s}_i^{nn}\rangle\}$) as a function of time. We find that the average of $\tilde{s}_i^{nn}$ has been first decreasing rapidly, and has then remained almost constant. This behavior is already clean from trends in the total volume of trade, since all weights have been rescaled and divided by $w_{tot}$. By contrast, the average of the randomized quantity $\langle\tilde{s}_i^{nn}\rangle$ displays a constant trend throughout the time interval considered, and its value is always significantly smaller than the empirical one. Thus, unlike the binary case, the null model does not reproduce the average values of the correlations considered, and does not capture their temporal evolution. A similar behavior is observed for the evolution of the standard deviation of the ANNS across vertices (Fig. 3b). In Fig. 3c we show the correlation coefficient between the empirical quantities $\{\tilde{s}_i^{nn}\}$ and $\{\tilde{s}_i\}$, whose value (fluctuating around $-0.4$) compactly summarizes the disassortativity of the noisy scatter plot that we have shown previously in Fig. 1, and the correlation coefficient between the randomized quantities $\{\langle\tilde{s}_i^{nn}\rangle\}$ and $\{\langle\tilde{s}_i\rangle\} = \{\tilde{s}_i\}$, which instead displays a different value close to $-1$ (due to the noise-free, even if much weaker, decrease of the randomized curve in Fig. 1). The discrepancy between the null model and the real network is finally confirmed by the small correlation between $\{\tilde{s}_i^{nn}\}$ and $\{\langle\tilde{s}_i^{nn}\rangle\}$ (Fig. 3d), which is in marked contrast with the perfect correlation between $\{k_i^{nn}\}$ and $\{\langle k_i^{nn}\rangle\}$ we found in the binary case.

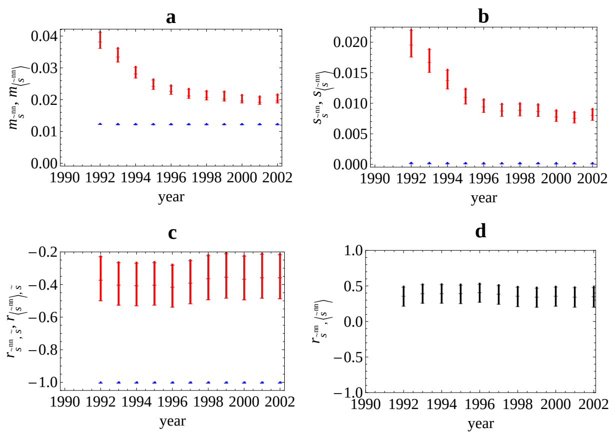


FIG. 3: Temporal evolution of the properties of the (rescaled) average nearest neighbor strength $\tilde{s}_i^{nn}$ in the 1992-2002 snapshots of the real weighted undirected ITN and of the corresponding maximum-entropy ensembles with specified strengths. **a)** average of $\tilde{s}_i^{nn}$ across all vertices (red: real, blue: randomized). **b)** standard deviation of $\tilde{s}_i^{nn}$ across all vertices (red: real, blue: randomized). **c)** correlation coefficient between $\tilde{s}_i^{nn}$ and $\tilde{s}_i$ (red: real, blue: randomized). **d)** correlation coefficient between $\tilde{s}_i^{nn}$ and $\langle\tilde{s}_i^{nn}\rangle$. The 95% confidence intervals of all quantities are represented as vertical bars.

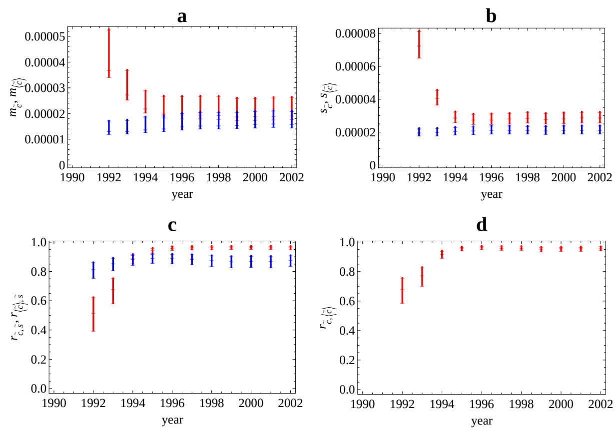


FIG. 4: Temporal evolution of the properties of the (rescaled) weighted clustering coefficient $\tilde{c}_i$ in the 1992-2002 snapshots of the real weighted undirected ITN and of the corresponding maximum-entropy ensembles with specified strengths. **a)** average of $\tilde{c}_i$ across all vertices (red: real, blue: randomized). **b)** standard deviation of $\tilde{c}_i$ across all vertices (red: real, blue: randomized). **c)** correlation coefficient between $\tilde{c}_i$ and $\tilde{s}_i$ (red: real, blue: randomized). **d)** correlation coefficient between $\tilde{c}_i$ and $\langle\tilde{c}_i\rangle$. The 95% confidence intervals of all quantities are represented as vertical bars.

In Fig. 4 we report a similar analysis for the evolution of the weighted clustering coefficient. We find that, despite the partial accordance of the real and randomized clustering profiles shown in Fig. 2, the average level of clustering of the real network is always higher than its randomized variant (Fig. 4a), even if the two values have become closer through time. The same is true for the standard deviation of the weighted clustering coefficient (Fig. 4b). We also find that the correlation coefficient between the empirical quantities $\{\tilde{c}_i\}$ and $\{\tilde{s}_i\}$ (Fig. 4c) has rapidly increased between the years 1992 and 1995 (from about 0.5 to more than 0.95) and has then remained stable in time. This indicates that the scatter plot shown in Fig. 2 for the year 2002 becomes noisier in the first snapshots of our time window, as we confirmed through an explicit inspection (not shown). By contrast, the correlation coefficient between the randomized quantities $\{\langle\tilde{c}_i\rangle\}$ and $\{\langle\tilde{s}_i\rangle\} = \{\tilde{s}_i\}$ displays much smaller variations about the value 0.85, and is therefore initially larger, and eventually smaller, than the corresponding empirical value. Finally, in Fig. 4d we show the correlation coefficient between $\{\tilde{c}_i\}$ and $\{\langle\tilde{c}_i\rangle\}$. The increasing trend confirms the growing agreement between the real and randomized clustering coefficients, already suggested by the previous plots. Note however that even two perfectly correlated lists of values (correlation coefficient equal to 1) are only equal if their averages are the same (otherwise they are simply proportional to each other). Thus large correlation coefficients between two quantities can only be interpreted in conjunction with a comparison of the average values of the same quantities. While in the binary case we simultaneously found perfect correlation and equal average values between real and randomized quantities [1], in this case we find large correlation but different average values, systematically confirming only a partial accordance between the real network and the null model.

## D. Edge weights

So far, in our weighted network analysis of world trade we considered the weighted counterparts (strengths, ANNS, clustering) of the topological properties we had studied in the binary case [1]. However, due to the larger number of degrees of freedom, in the weighted case there are additional quantities to study which have no binary analogue. In particular, it is important to understand the effect that the enforcement of local constraints (strength sequence) has on the weights of the network, as well as on its purely binary topology.

To this end, we compare the empirical weight distribution with the expected one. Importantly, one should not confuse the expected weight distribution with the distribution of expected weights. In the spirit of our analysis, the empirical network (and so its weight distribution) is regarded as a particular possible realization of the null model with given strengths, and the comparison with the expected properties aims at assessing how unlikely that particular realization is. Therefore the observed number of edges with weight equal to $w$ (i.e. the empirical weight distribution) should be compared with the expected number of such edges in a single realization

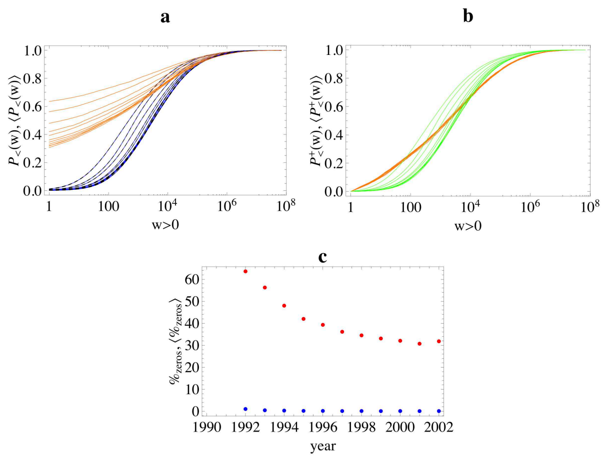


FIG. 5: Edge weights in the weighted undirected ITN. **a)** cumulative distributions of edge weights in the years 1992 (top curves) to 2002 (bottom curves). Orange: real network; blue: expectation for the maximum-entropy ensemble with specified strengths. **b)** same as the previous panel, but excluding zero weights (missing links). Orange: real network; green: randomization. **c)** percentage of missing links as a function of time. Red: real network; blue: randomization.

(the expected weight distribution), rather than with the number of edges whose expected weight across realizations is equal to $w$ (the distribution of expected weights). The difference between the two expected quantities is evidenced by the fact that the expected edge weight between vertices is always positive (see Appendix A), whereas in a single realization there are a number of zero-weight edges (i.e. missing links).

In Fig. 5a we therefore compare the cumulative distribution of observed weights $P_<(w)$ (the fraction of edge weights smaller than $w$) with the expected number $\langle P_<(w)\rangle$ (see Appendix A), both including missing links ($w = 0$) and therefore normalized to the number of pairs of vertices. As an alternative, in Fig. 5b we also compare the cumulative distribution of positive weights $P^+_<(w)$ (which excludes missing links and is therefore normalized to the total number of links) with the expected number $\langle P^+_<(w)\rangle$ (see Appendix A). We find that, for all years in our time window, the real distributions are always different from the expected ones. To rigorously confirm this, we have performed Kolmogorov-Smirnov and Lilliefors tests and for all years we always had to reject the hypothesis that real and expected distributions are the same (5% significance level). For the positive weight distributions $P^+_<(w)$ and $\langle P^+_<(w)\rangle$ we also separately tested the hypothesis of the log-normality of the distributions, and again we always had to reject it (5% significance level).

The above results, besides highlighting large differences in the weighted structure of real and randomized networks, also convey important information about remarkable deviations in their topology. The largest difference between the curves $P_<(w)$ and $\langle P_<(w)\rangle$ is found at $w = 0$, and the corresponding points $P_<(0)$ and $\langle P_<(0)\rangle$ represent the fractions $\%_{zeros}$ and $\langle\%_{zeros}\rangle$ of zero weights (missing links) in the network. In Fig. 5c we show the evolution of these fractions over time. We find that the fraction of missing links in the real network decreases in time over the time interval considered (i.e. the link density increases), but its value is always much larger than the corresponding (vanishing) expected value. Thus, despite it is usually considered a very dense graph, with more links per node than most other real-world networks, we find that the ITN turns out to be surprisingly sparser than random weighted networks with the same strength sequence. This fixes a previously unavailable benchmark for the density of the empirical ITN, and implies that the high percentage of missing trade relations among world countries is not explained by size effects (i.e. the total trade value of all countries).

### E. Commodity-specific weighted undirected networks

We now focus on the disaggregated commodity-specific versions of the weighted undirected ITN, representing the trade of single classes of products. We therefore repeat the previous analyses after setting $\mathbf{W} \equiv \mathbf{W}^c$ for various individual commodities $c > 0$. As we did for the binary case [1], we show our results for a subset of 6 commodities taken from the top 14 categories, namely the two commodities with the smallest traded volume ($c = 93, 9$), two ones with intermediate volume ($c = 39, 90$), the one with the largest volume ($c = 84$), plus the aggregation of all the top 14 commodities (similar results hold also for the other commodities). Together with the completely aggregated data ($c = 0$) considered above, this dataset consists of 7 networks with increasing trade volume and level of aggregation.

In Fig. 6, we show the scatter plot of the average nearest neighbor strength as a function of the strength. Similarly, in Fig. 7, we report the scatter plot for the weighted clustering coefficient. Both are shown for the 2002 snapshots of the 6 commodity-specific networks. When compared with the aggregated network (shown previously in Figs. 1 and 2), these results lead to interesting conclusions. In general, as happens in the binary case [1], we find that commodities with a lower traded volume feature more dispersed scatter plots, with larger fluctuations of the empirical data around the average trend. The effect is more pronounced here than in the binary case. However, while in the latter the real networks are always well reproduced by the null model, in the weighted case the disagreement between empirical and randomized data remains strong across different levels of commodity aggregation. Moreover, the weighted clustering coefficient is the quantity that displays the largest differences between aggregated and disaggregated networks. We see that, for all commodity classes considered, the observed weighted clustering coefficient is generally larger

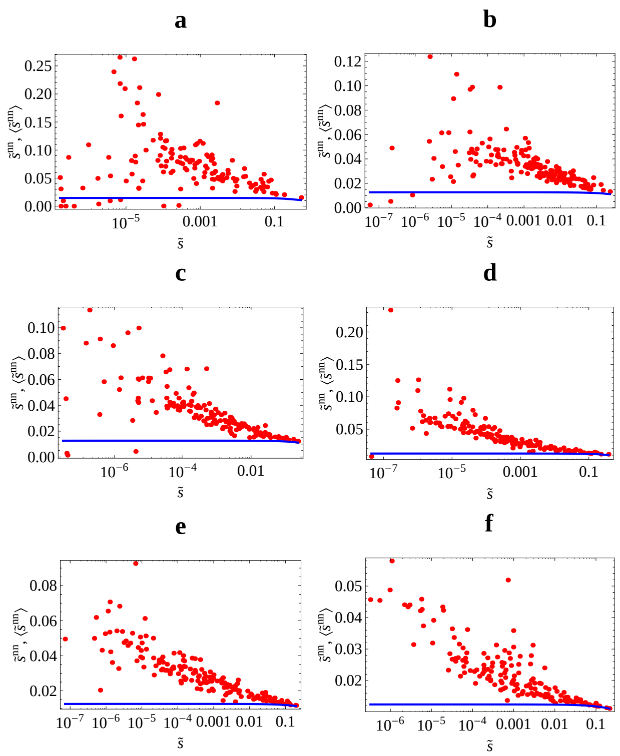


FIG. 6: Average nearest neighbor strength $\tilde{s}_i^{nn}$ versus strength $\tilde{s}_i$ in the 2002 snapshots of the commodity-specific (disaggregated) versions of the real weighted undirected ITN (red points), and corresponding average over the maximum-entropy ensemble with specified strengths (blue curve). **a)** commodity 93; **b)** commodity 09; **c)** commodity 39; **d)** commodity 90; **e)** commodity 84; **f)** aggregation of the top 14 commodities (see Ref. [1] for details). From a) to f), the intensity of trade and level of aggregation increases.

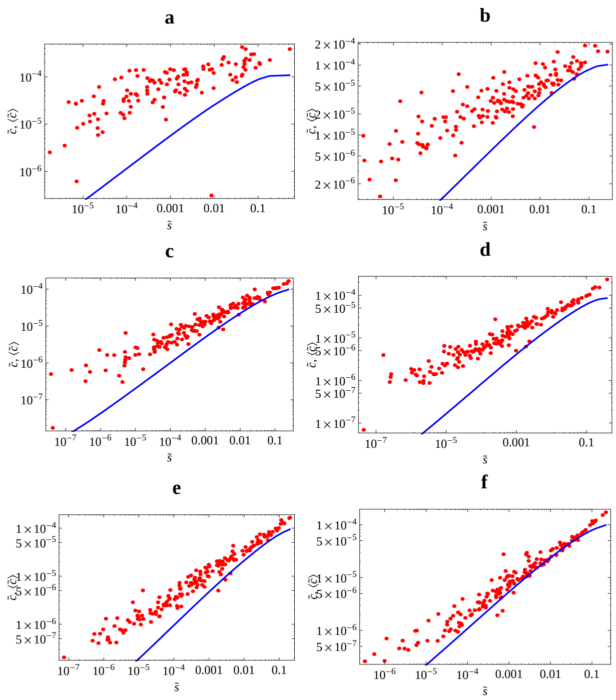


FIG. 7: Weighted clustering coefficient $\tilde{c}_i$ versus strength $\tilde{s}_i$ in the 2002 snapshots of the commodity-specific (disaggregated) versions of the real weighted undirected ITN (red points), and corresponding average over the maximum-entropy ensemble with specified strengths (blue curve). **a)** commodity 93; **b)** commodity 09; **c)** commodity 39; **d)** commodity 90; **e)** commodity 84; **f)** aggregation of the top 14 commodities (see Ref. [1] for details). From a) to f), the intensity of trade and level of aggregation increases.

than its randomized counterpart. However, the deviation is larger for sparser commodities, and decreases as commodity classes with larger trade volumes and higher levels of aggregation are considered. This shows that the partial agreement between real and randomized networks in the completely aggregated case (see Fig. 2) is not robust to disaggregation. In other words, the accordance between empirical data and null model, which according to our discussion in Section II C is already incomplete in the aggregated case, becomes even worse for sparser commodity-specific networks.

The above results confirm that, unlike the binary case, the properties of the weighted undirected version of the ITN are not completely reproduced by simply controlling for the local properties. The presence of higher-order mechanisms is required as an explanation for the onset and evolution of the observed patterns. This result holds across different years and is enhanced as lower levels of commodity aggregation are considered. This shows that a weighted network approach to the analysis of international trade conveys additional information with respect to traditional economic studies that describe trade in terms of local properties alone (total trade, openness, etc.) [5]. Interestingly, a major deviation between the real network and the null model is in the topology implied by local constraints. This confirms, from a different point of view, that in order to properly understand the structure of the international trade system is essential to reproduce its binary topology, even if one is interested in a weighted description.

## III. THE ITN AS A WEIGHTED DIRECTED NETWORK

We now turn to the weighted directed analysis of the ITN. A single graph $\mathbf{G}$ in the ensemble of weighted directed networks is completely specified by its generic weight matrix $\mathbf{W}$ which is in general not symmetric, and whose entry $w_{ij}$ represents the intensity of the directed link from vertex $i$ to vertex $j$ ($w_{ij} = 0$ if no directed link is there). The binary adjacency $\mathbf{A}$, with entries $a_{ij} = \Theta(w_{ij})$, is in general not symmetric as well. The *out-strength sequence* $\{s_i^{out}\}$ and the *in-strength sequence* $\{s_i^{in}\}$ represent the local constraints $\{C_a\}$ in the weighted directed case [1]. The randomization method [2] yields the expectation value $\langle X\rangle$ of a property $X$ across the maximally random ensemble of weighted directed graphs with in-strength and out-strength sequences equal to the observed ones (see Appendix B). The quantities $\{s_i^{out}\}$ and $\{s_i^{in}\}$ (or combinations of them) are now the natural independent variables against which other properties can be visualized in both the real and randomized case, since their expected value coincides with the observed one by construction. As for the weighted undirected case, we will consider the rescaled weights $\tilde{w}_{ij} = w_{ij}/w_{tot}$ in order to wash away trends due to an overall change in the volume of trade across different years. Correspondingly we consider the rescaled strengths

$$\tilde{s}_i^{out} \equiv \sum_{j\neq i} \tilde{w}_{ij} = \frac{\tilde{s}_i^{out}}{w_{tot}} \quad (5)$$

$$\tilde{s}_i^{in} \equiv \sum_{j\neq i} \tilde{w}_{ji} = \frac{\tilde{s}_i^{in}}{w_{tot}} \quad (6)$$

$$(7)$$

(where $w_{tot} = \sum_i \sum_{j\neq i} w_{ij}$) and we analogously use $\tilde{w}_{ij}$ instead of $w_{ij}$ in the definition of all quantities. Note that $w_{tot} = \sum_i s_i^{in} = \sum_i s_i^{out}$, and since $\langle s_i^{in}\rangle = s_i^{in}$ and $\langle s_i^{out}\rangle = s_i^{out}$ we have

$$\langle w_{tot}\rangle = \sum_i \langle s_i^{in}\rangle = \sum_i s_i^{in} = w_{tot} \quad (8)$$

Therefore, as for the undirected case, the expected value of $w_{tot}$ coincides with its empirical value, and the total weight can therefore be safely used to rescale the weights of both real and randomized networks. As usual, we first consider the aggregated snapshot for year 2002 in more detail, then discuss the temporal evolution of the results, and finally perform a study of disaggregated networks.

### A. Directed average nearest neighbor strengths

We consider four generalizations of the definition of the average nearest neighbor strength of a vertex in a directed weighted network:

$$\tilde{s}_i^{in/in} \equiv \frac{\sum_{j\neq i} a_{ji}\tilde{s}_j^{in}}{k_i^{in}} = \frac{\sum_{j\neq i}\sum_{k\neq j} a_{ji}\tilde{w}_{kj}}{\sum_{j\neq i} a_{ji}} \quad (9)$$

$$\tilde{s}_i^{in/out} \equiv \frac{\sum_{j\neq i} a_{ji}\tilde{s}_j^{out}}{k_i^{in}} = \frac{\sum_{j\neq i}\sum_{k\neq j} a_{ji}\tilde{w}_{jk}}{\sum_{j\neq i} a_{ji}} \quad (10)$$

$$\tilde{s}_i^{out/in} \equiv \frac{\sum_{j\neq i} a_{ij}\tilde{s}_j^{in}}{k_i^{out}} = \frac{\sum_{j\neq i}\sum_{k\neq j} a_{ij}\tilde{w}_{kj}}{\sum_{j\neq i} a_{ij}} \quad (11)$$

$$\tilde{s}_i^{out/out} \equiv \frac{\sum_{j\neq i} a_{ij}\tilde{s}_j^{out}}{k_i^{out}} = \frac{\sum_{j\neq i}\sum_{k\neq j} a_{ij}\tilde{w}_{jk}}{\sum_{j\neq i} a_{ij}} \quad (12)$$

Indirect interactions due to chains of length two (products of the type $a_{ij}\tilde{w}_{kl}$) contribute to the above quantities. A fifth aggregated quantity, which is the natural analogue of the undirected ANNS, is based on the (rescaled) total strength $\tilde{s}_i^{tot} \equiv \tilde{s}_i^{in} + \tilde{s}_i^{out}$:

$$\tilde{s}_i^{tot/tot} \equiv \frac{\sum_{j\neq i}(a_{ij}+a_{ji})\tilde{s}_j^{tot}}{k_i^{tot}} \quad (13)$$

We start by considering the latter. In Fig. 8 we show $\tilde{s}_i^{tot/tot}$, together with its randomized value $\langle\tilde{s}_i^{tot/tot}\rangle$ (obtained as in Appendix B), as a function of $\tilde{s}_i^{tot}$ in the aggregated snapshot for year 2002. There are no significant differences with respect to Fig. 1, apart from a "double" series of randomized values due to the two possible directions (the terms $a_{ij}$ and $a_{ji}$) that contribute to the definition of $\tilde{s}_i^{tot/tot}$ in Eq. (13). Thus we still observe a disassortative behavior in the empirical network, which is not paralleled by the null model.

We now turn to the four directed versions of the ANNS defined in Eqs.(9)-(12), as well as their randomized values (see Appendix B). As shown in Fig. 9, we find that the four empirical quantities all display the same disassortative trend, whereas the four randomized ones are always approximately flat (and no longer switch between two trends as in Fig. 8). These results show that, as in the undirected representation, the correlation properties of the directed weighted ITN deviate significantly from the ones displayed by the null model with specified strength sequences. In particular, the pronounced disassortativity of the real network is a true signature of negative correlations between the total trade values (in any direction) of neighboring countries, even after controlling for the heterogeneities in the total trade values themselves. This is in marked contrast with the binary case, where we showed that the observed disassortativity is completely explained by controlling for the empirical degree sequence [1].

### B. Directed weighted clustering coefficients

The four weighted versions of the *inward*, *outward*, *cyclic* and *middleman* directed clustering coefficients considered in Ref. [1] read [4]

$$\tilde{c}_i^{in} \equiv \frac{\sum_{j\neq i}\sum_{k\neq i,j}(\tilde{w}_{ki}\tilde{w}_{ji}\tilde{w}_{jk})^{1/3}}{k_i^{in}(k_i^{in}-1)} \quad (14)$$

$$\tilde{c}_i^{out} \equiv \frac{\sum_{j\neq i}\sum_{k\neq i,j}(\tilde{w}_{ik}\tilde{w}_{jk}\tilde{w}_{ij})^{1/3}}{k_i^{out}(k_i^{out}-1)} \quad (15)$$

$$\tilde{c}_i^{cyc} \equiv \frac{\sum_{j\neq i}\sum_{k\neq i,j}(\tilde{w}_{ij}\tilde{w}_{jk}\tilde{w}_{ki})^{1/3}}{k_i^{in}k_i^{out}-k_i^{\leftrightarrow}} \quad (16)$$

$$\tilde{c}_i^{mid} \equiv \frac{\sum_{j\neq i}\sum_{k\neq i,j}(\tilde{w}_{ik}\tilde{w}_{ji}\tilde{w}_{jk})^{1/3}}{k_i^{in}k_i^{out}-k_i^{\leftrightarrow}} \quad (17)$$

The above quantities capture indirect interactions of length 3 according to their directionality, appearing as products of the type $\tilde{w}_{ij}\tilde{w}_{kl}\tilde{w}_{mn}$. A fifth measure aggregates all directions:

$$\tilde{c}_i^{tot} \equiv \frac{\sum_{j\neq i}\sum_{k\neq i,j}(\tilde{w}_{ij}^{1/3}+\tilde{w}_{ji}^{1/3})(\tilde{w}_{jk}^{1/3}+\tilde{w}_{kj}^{1/3})(\tilde{w}_{ki}^{1/3}+\tilde{w}_{ik}^{1/3})}{2\left[k_i^{tot}(k_i^{tot}-1)-2k_i^{\leftrightarrow}\right]}$$

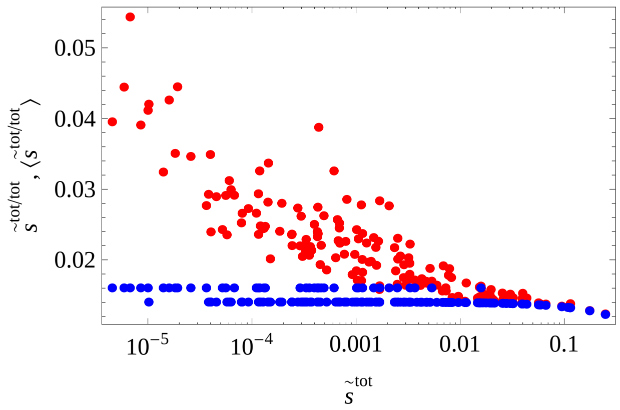


FIG. 8: Total average nearest neighbor strength $\tilde{s}_i^{tot/tot}$ versus total strength $\tilde{s}_i^{tot}$ in the 2002 snapshot of the real weighted directed ITN (red points), and corresponding average over the maximum-entropy ensemble with specified out-strengths and in-strengths (blue curve).

We show the latter in Fig. 10, and the four directed quantities defined in Eqs.(14)-(17) in Fig. 11. All properties are shown together with their randomized values (see Appendix B), and plotted against the natural independent variables (or combinations of them). Again, there is no significant difference with respect to the weighted undirected plot (Fig. 2), apart from the switching behavior of $\langle \tilde{c}_i^{tot} \rangle$ between two trends as already discussed for $\langle \tilde{s}_i^{tot/tot} \rangle$. We find an approximate agreement between real and randomized clustering profiles.

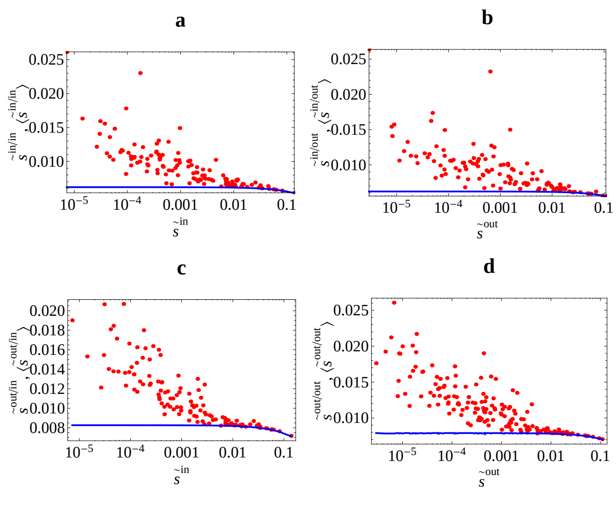


FIG. 9: Directed average nearest neighbor strengths versus vertex strengths in the 2002 snapshot of the real weighted directed ITN (red points), and corresponding averages over the maximum-entropy ensemble with specified out-strengths and in-strengths (blue curves). **a)** $\tilde{s}_i^{in/in}$ versus $\tilde{s}_i^{in}$; **b)** $\tilde{s}_i^{in/out}$ versus $\tilde{s}_i^{in}$; **c)** $\tilde{s}_i^{out/in}$ versus $\tilde{s}_i^{out}$; **d)** $\tilde{s}_i^{out/out}$ versus $\tilde{s}_i^{out}$.

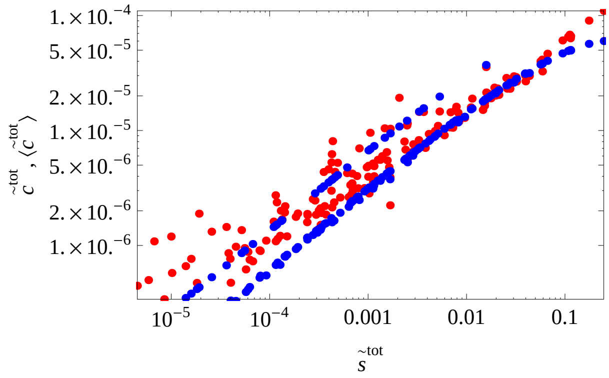


FIG. 10: Total weighted clustering coefficient $\tilde{c}_i^{tot}$ versus total strength $\tilde{s}_i^{tot}$ in the 2002 snapshot of the real weighted directed ITN (red points), and corresponding average over the maximum-entropy ensemble with specified out-strengths and in-strengths (blue curve).

### C. Evolution of weighted directed properties

We now study the temporal evolution of the structural properties considered. Figure 12 reports the average, standard deviation, and correlation coefficients for $\tilde{s}_i^{tot/tot}$ as a function of time, and Fig. 13 reports (for brevity) only the average of the four directed variants $\tilde{s}_i^{in/in}$, $\tilde{s}_i^{in/out}$, $\tilde{s}_i^{out/in}$, $\tilde{s}_i^{out/out}$. We find that the detailed description offered by the directed structural properties portrays a different picture with respect to the undirected results shown in Fig. 3. In particular, we find that the empirical trends are not always decreasing and the randomized trends are not always constant,

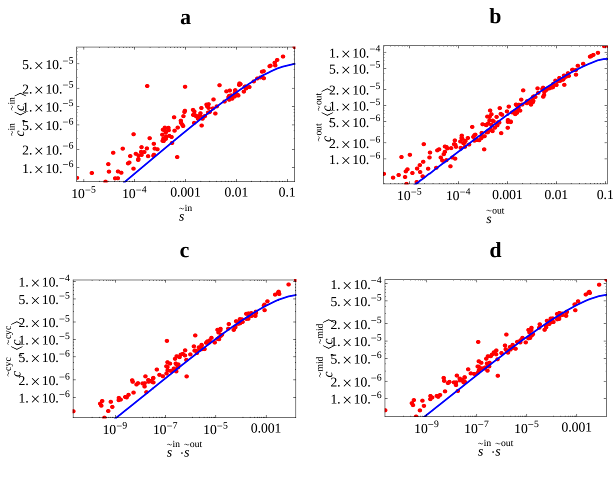


FIG. 11: Weighted clustering coefficients versus vertex strengths in the 2002 snapshot of the real weighted directed ITN (red points), and corresponding averages over the maximum-entropy ensemble with specified out-strengths and in-strengths (blue curves). **a)** $\tilde{c}_i^{in}$ versus $\tilde{s}_i^{in}$; **b)** $\tilde{c}_i^{out}$ versus $\tilde{s}_i^{out}$; **c)** $\tilde{c}_i^{cyc}$ versus $\tilde{s}_i^{in} \cdot \tilde{s}_i^{out}$; **d)** $\tilde{c}_i^{mid}$ versus $\tilde{s}_i^{in} \cdot \tilde{s}_i^{out}$.

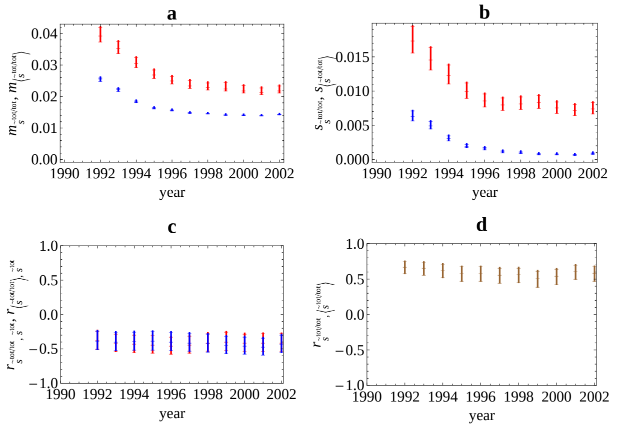


FIG. 12: Temporal evolution of the properties of the (rescaled) total average nearest neighbor strength $\tilde{s}_i^{tot/tot}$ in the 1992-2002 snapshots of the real weighted directed ITN and of the corresponding maximum-entropy ensembles with specified out-strengths and in-strengths. **a)** average of $\tilde{s}_i^{tot/tot}$ across all vertices (red: real, blue: randomized). **b)** standard deviation of $\tilde{s}_i^{tot/tot}$ across all vertices (red: real, blue: randomized). **c)** correlation coefficient between $\tilde{s}_i^{tot/tot}$ and $\tilde{s}_i^{tot}$ (red: real, blue: randomized). **d)** correlation coefficient between $\tilde{s}_i^{tot/tot}$ and $\langle \tilde{s}_i^{tot/tot} \rangle$. The 95% confidence intervals of all quantities are represented as vertical bars.

in contrast with what previously observed for the undirected ANNS. Both the empirical and randomized values of $\tilde{s}_i^{tot/tot}$ (Fig. 12a) and $\tilde{s}_i^{out/in}$ (Fig. 13c) display decreasing averages, whereas $\tilde{s}_i^{in/in}$ (Fig. 13a) and $\tilde{s}_i^{in/out}$ (Fig. 13b) display constant randomized values and first increasing, then slightly decreasing empirical values. In addition, $\tilde{s}_i^{out/out}$ (Fig. 13d) displays a different behavior

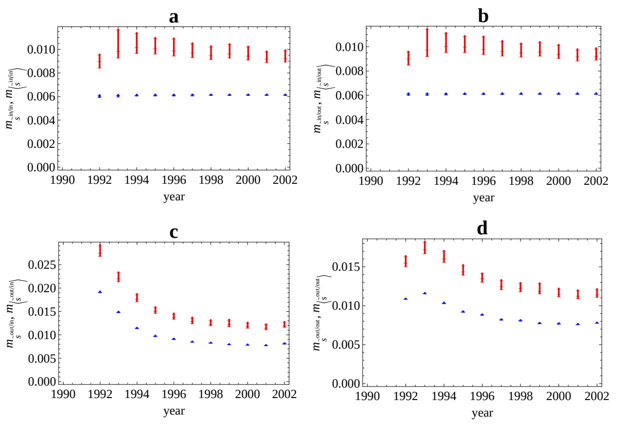


FIG. 13: Averages and their 95% confidence intervals (across all vertices) of the directed average nearest neighbor strengths in the 1992-2002 snapshots of the real weighted directed ITN (red), and corresponding averages over the maximum-entropy ensemble with specified out-strengths and in-strengths (blue). **a)** $\tilde{s}_i^{in/in}$; **b)** $\tilde{s}_i^{in/out}$; **c)** $\tilde{s}_i^{out/in}$; **d)** $\tilde{s}_i^{out/out}$.

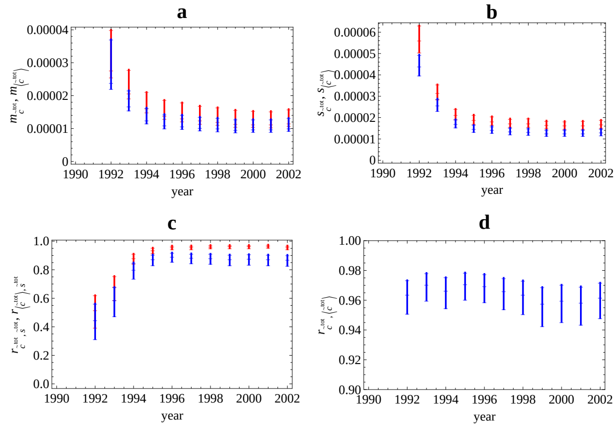


FIG. 14: Temporal evolution of the properties of the (rescaled) total weighted clustering coefficient $\tilde{c}_i^{tot}$ in the 1992-2002 snapshots of the real weighted directed ITN and of the corresponding maximum-entropy ensembles with specified out-strengths and in-strengths. **a)** average of $\tilde{c}_i^{tot}$ across all vertices (red: real, blue: randomized). **b)** standard deviation of $\tilde{c}_i^{tot}$ across all vertices (red: real, blue: randomized). **c)** correlation coefficient between $\tilde{c}_i^{tot}$ and $\tilde{s}_i^{tot}$ (red: real, blue: randomized). **d)** correlation coefficient between $\tilde{c}_i^{tot}$ and $\langle \tilde{c}_i^{tot} \rangle$. The 95% confidence intervals of all quantities are represented as vertical bars.

where both real and randomized averages first increase and then decrease. These fine-level differences are all washed away in the undirected description considered in Section II, signaling a loss of information like the one we also observed in the binary case [1]. However, while in the latter the null model was always in agreement with the empirical data, here we always observe large deviations. In particular, the averages and standard deviations of all empirical quantities are different from their

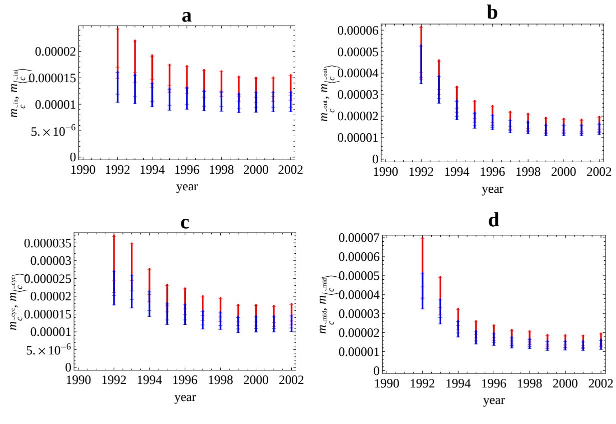


FIG. 15: Averages and their 95% confidence intervals (across all vertices) of the directed weighted clustering coefficients in the 1992-2002 snapshots of the real weighted directed ITN (red), and corresponding averages over the maximum-entropy ensemble with specified out-strengths and in-strengths (blue). **a)** $\tilde{c}_i^{in}$; **b)** $\tilde{c}_i^{out}$; **c)** $\tilde{c}_i^{cyc}$; **d)** $\tilde{c}_i^{mid}$.

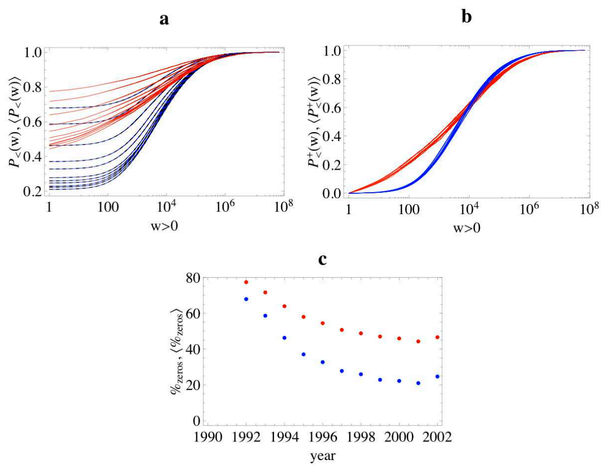


FIG. 16: Edge weights in the weighted directed ITN (red: real network, blue: expectation for the maximum-entropy ensemble with specified out-strengths and in-strengths). **a)** cumulative distributions of edge weights in the years 1992 (top curves) to 2002 (bottom curves). **b)** same as the previous panel, but excluding zero weights (missing links). **c)** percentage of missing links as a function of time.

randomized counterparts, and the analysis of the correlation coefficients confirms that the disassortative behavior of the real network is robust in time, and its intensity is systematically not reproduced by the null model.

Different considerations apply to the evolution of the weighted directed clustering coefficients $\tilde{c}_i^{tot}$, $\tilde{c}_i^{in}$, $\tilde{c}_i^{out}$, $\tilde{c}_i^{cyc}$ and $\tilde{c}_i^{mid}$, shown in Figs. 14 and 15. In this case we find that the undirected trend we observed in Fig. 4 is still not representative of the individual trends of the directed coefficients studied here. However, the empirical and randomized values of the latter are found to be closer here than in the undirected case, and to follow similar temporal behaviors. The null model is however only marginally consistent with the real network, and the knowledge of the strength sequences remains of limited informativeness.

### D. Directed edge weights

As we did in Section II D for the weighted undirected case, we now study the consequences that the specification of the in- and out-strength sequences has on the weights of the network and on its density.

In Fig. 16a we show the cumulative distribution of observed weights $P_<(w)$ (including missing links with $w = 0$) and its randomized counterpart $\langle P_<(w)\rangle$ (see Appendix B). Similarly, in Fig. 16b we show the cumulative distribution of observed positive weights $P^+_<(w)$ (excluding missing links) and the randomized one $\langle P^+_<(w)\rangle$ (see Appendix B). As in the undirected case, we find that the empirical distributions are always different from the randomized ones, and we confirmed that the hypothesis of equality of real and expected distributions is always rejected by both Kolmogorov-Smirnov and Lilliefors tests (5% significance level). Similarly, the hypothesis of log-normality of the positive weight distributions $P^+_<(w)$ and $\langle P^+_<(w)\rangle$ is always rejected (5% significance level).

In this case too, we can monitor the important difference between the topological density of the real and randomized ITN by plotting the fractions of missing links $\%_{zeros} = P_<(0)$ and $\langle\%_{zeros}\rangle = \langle P_<(0)\rangle$ as a function of time (Fig. 16c). Even if the difference is smaller than in the undirected case, we can confirm on a directed basis that, despite it is usually considered a dense graph, the observed ITN is surprisingly sparser than random directed weighted networks with the same in- and out-strength sequences. Thus the density of (missing) links in the real trade network is not accounted for by size considerations (total imports and total exports of world countries).

### E. Commodity-specific weighted directed networks

We finally come to the analysis of disaggregated commodity-specific representations of the weighted directed ITN. We show results for the usual subset of 6 commodity classes ordered by increasing trade intensity ad level of commodity aggregation, to which we can add the completely aggregated case already discussed (again, we found similar results for all commodities).

Figures 17 and 18 report the total average nearest neighbor strength and total weighted clustering coefficient as functions of the total strength, for the 6 selected commodity classes in year 2002. The corresponding plots for the aggregated networks were shown previously in Figs. 8 and 10. We find once again that, as more intensely traded commodities and higher levels of aggregation are considered, the empirical data become less scattered around their average trend. In this case, the same effect holds also for the randomized data. As for the weighted undirected case, and unlike the binary representation, there is no agreement between empirical networks and the null model. The accordance becomes even worse as commodity classes with smaller trade volume and lower level of aggregation are considered.

The above results extend to the directed case what we found in the analysis of weighted undirected properties. In particular, unlike the binary case, the knowledge of local properties conveys only limited information about the actual structure of the network. Higher-order properties are not explained by local constraints, and indirect interactions cannot be decomposed to direct ones. This holds irrespective of the commodity aggregation level and the particular year considered. This implies that a weighted network approach captures more information than simpler analyses focusing on country-specific local properties. Moreover, simple purely topological properties such as link density are not reproduced by the null model. This implies that, even in weighted analyses, the binary structure is an important property to explain, because it

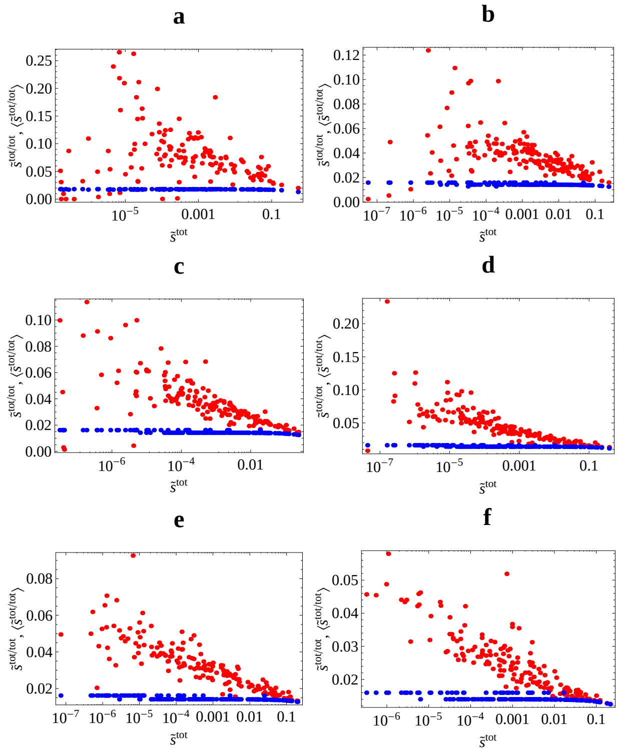


FIG. 17: Total average nearest neighbor strength $\tilde{s}_i^{tot/tot}$ versus total strength $\tilde{s}_i^{tot}$ in the 2002 snapshots of the commodity-specific (disaggregated) versions of the real weighted directed ITN (red points), and corresponding average over the maximum-entropy ensemble with specified out-strengths and in-strengths (blue curve). **a)** commodity 93; **b)** commodity 09; **c)** commodity 39; **d)** commodity 90; **e)** commodity 84; **f)** aggregation of the top 14 commodities (see Ref. [1] for details). From a) to f), the intensity of trade and level of aggregation increases.

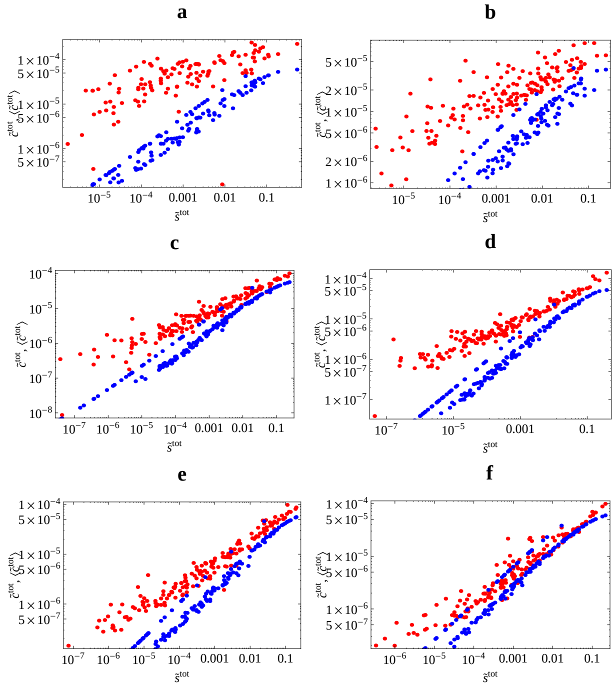


FIG. 18: Total weighted clustering coefficient $\tilde{c}_i^{tot}$ versus total strength $\tilde{s}_i^{tot}$ in the 2002 snapshots of the commodity-specific (disaggregated) versions of the real weighted directed ITN (red points), and corresponding average over the maximum-entropy ensemble with specified our-strengths and in-strengths (blue curve). **a)** commodity 93; **b)** commodity 09; **c)** commodity 39; **d)** commodity 90; **e)** commodity 84; **f)** aggregation of the top 14 commodities (see Ref. [1] for details). From a) to f), the intensity of trade and level of aggregation increases.

is responsible of major departures of the empirical network from the null model. Therefore, both binary and weighted analyses highlight, for completely different reasons, the importance of reproducing the ITN topology and devoting it more consideration in models of trade.

## IV. CONCLUSIONS

In this paper and in the preceding one [1] we have derived a series of results about the structure of the ITN and the role that local topological properties have in constraining it. Our findings are *a priori* unpredictable without a comparison with a null model, and can be summarized as follows.

In the binary description (both in the directed and undirected cases), we found that specifying the degree sequence(s) (a first-order topological property) is enough to explain all higher-order properties [1]. This result has two consequences. First, it implies that all the observed patterns (disassortativity, clustering, etc.) should not be interpreted as genuine higher-order stylized facts and do not require additional explanations besides those accounting for the different specific numbers of trade partners of all countries. Second, it indicates that the degree sequence encodes virtually all the binary information and is therefore a key structural property that economic models of trade should try to explain in detail.

By contrast, in the weighted description (again, both in the directed and undirected cases) specifying the strength sequence(s) is *not* enough in order to reproduce the other properties of the network. Therefore the knowledge of total trade volumes of all countries is of limited informativeness. A weighted network description of trade, by taking into account indirect interactions besides direct ones, succeeds in conveying additional, nontrivial information with respect to standard economic analyses that explain international trade in terms of local country-specific properties only. In particular, in this case the disassortative character of the network and the high level of clustering cannot be simply traced back to the observed local trade volumes and requires additional explanations. Moreover, the purely binary topology of the real trade network is different and sparser (despite the ITN is traditionally considered a very dense network) than the one predicted by the null model with the same strength sequence.

Our results bear important consequences for the theory of international trade. The most commonly used modeling framework, i.e. that of gravity models [6, 7], relies on the assumption that the intensity of trade between countries $i$ and $j$ depends only on individual properties of $i$ and $j$ (e.g., their GDP) and on additional pairwise quantities relevant to $i$ and $j$ alone (the distance between them plus other factors either favoring or impeding trade). The irreducibility of weighted indirect interactions to direct ones, that we have shown above, implies that even if gravity models succeed in reproducing the magnitude of isolated interactions, they fail to capture the complexity of longer chains of relationships in the network. Moreover, as we have shown, much of the deviation between real and randomized networks in the weighted case is due to differences in the bare topology. This means that, in order to successfully reproduce the weighted properties of the ITN, it is essential to correctly replicate its binary structure, confirming (from a completely different perspective) the importance of the latter. This explains why in other studies the weighted properties of the aggregated ITN have been replicated by specifying the strength and the degree of all vertices simultaneously [8]. Even if it is not the focus of the present work, the effects of a simultaneous specification of the strength sequence and of the degree sequence can be studied in more detail applying the same maximum-likelihood method used here [2] by exploiting the analytical results available for the corresponding maximum-entropy ensemble of weighted graphs [9]. In general, our results indicate that theories and models of international trade are incomplete if they only focus on bilateral trade volumes and local weighted properties as in the case of gravity models, and if they do not include the binary topology of the ITN among the main empirical properties to replicate.

**Acknowledgments**

D.G. acknowledges financial support from the European Commission 6th FP (Contract CIT3-CT-2005-513396), Project: DIME - Dynamics of Institutions and Markets in Europe.

## APPENDIX A: WEIGHTED UNDIRECTED PROPERTIES

In the weighted undirected case, each graph $\mathbf{G}$ is completely specified by its (symmetric) non-negative weight matrix $\mathbf{W}$. The entries $w_{ij}$ of this matrix are integer-valued, since so are the trade values we consider [1]. The randomization method we are adopting [2] proceeds by specifying the strength sequence as the constraint: $\{C_a\} = \{s_i\}$. The Hamiltonian therefore reads

$$H(\mathbf{W}) = \sum_i \theta_i s_i(\mathbf{W}) = \sum_i \sum_{j<i} (\theta_i + \theta_j) w_{ij} \qquad \text{(A1)}$$

and one can show [9] that this allows to write the graph probability as

$$P(\mathbf{W}) = \prod_i \prod_{j<i} q_{ij}(w_{ij}) \qquad \text{(A2)}$$

where

$$q_{ij}(w) = (x_i x_j)^w (1 - x_i x_j) \qquad \text{(A3)}$$

(with $x_i \equiv e^{-\theta_i}$) is the probability that a link of weight $w$ exists between vertices $i$ and $j$ in the maximum-entropy ensemble of weighted undirected graphs, subject to specifying a given strength sequence as the constraint. If the latter is chosen to be the empirical strength sequence $\{s_i(\mathbf{W}^*)\}$ of the particular real network $\mathbf{W}^*$, then Eq. (A3) yields the exact value of the connection probability in the ensemble of randomized weighted networks with the same average strength sequence as the empirical one, provided that the parameters $\{x_i\}$ are set to the values that maximize the likelihood $P(\mathbf{W}^*)$ [2]. These values are the solution of the following set of $N$ coupled nonlinear equations:

$$\langle s_i \rangle = \sum_{j \neq i} \frac{x_i x_j}{1 - x_i x_j} = s_i(\mathbf{W}^*) \qquad \forall i \qquad \text{(A4)}$$

Once the values $\{x_i\}$ are found, they are inserted into Eq. (A3) which allows to easily compute the expectation value $\langle X \rangle$ of any topological property $X$ analytically, without generating the randomized networks explicitly [2]. Equation (A4) shows that, by construction, the strengths of all vertices are special local quantities whose expected and empirical values are exactly equal: $\langle s_i \rangle = s_i$. The expectation values of the higher-order topological properties considered in the main text can be obtained as in Table I. The expressions are derived exploiting the fact that $\langle w_{ij} \rangle = \sum_w w q_{ij}(w) = x_i x_j / (1 - x_i x_j)$, and that different pairs of vertices are statistically independent, which implies $\langle w_{ij} w_{kl} \rangle = \langle w_{ij} \rangle \langle w_{kl} \rangle$ if $(i-j)$ and $(k-l)$ are distinct pairs of vertices, whereas $\langle w_{ij} w_{kl} \rangle = \langle w_{ij}^2 \rangle$ if $(i-j)$ and $(k-l)$ are the same pair of vertices. The expected value of the power of the weight between vertices $i$ and $j$ is calculated as follows:

$$\langle w_{ij}^\alpha \rangle \equiv \sum_w w^\alpha q_{ij}(w) = (1 - x_i x_j) \mathrm{Li}_{-\alpha}(x_i x_j) \qquad \text{(A5)}$$

where $\mathrm{Li}_n(z)$ denotes the Polylogarithm function defined as

$$\mathrm{Li}_n(z) \equiv \sum_{l=1}^{\infty} \frac{z^l}{l^n} \qquad \text{(A6)}$$

The adjacency matrix representing the existence of a link (irrespective of its intensity) between vertex $i$ and

| **Empirical undirected properties** | **Expected undirected properties** |
|---|---|
| $w_{ij}$ | $\langle w_{ij}\rangle = \frac{x_i x_j}{1-x_i x_j}$ |
| $\tilde{w}_{ij} = \frac{w_{ij}}{w_{tot}}$ | $\langle \tilde{w}_{ij}\rangle = \frac{\langle w_{ij}\rangle}{\langle w_{tot}\rangle} = \frac{\langle w_{ij}\rangle}{w_{tot}}$ |
| $a_{ij} = \Theta(w_{ij})$ | $\langle a_{ij}\rangle = p_{ij} = x_i x_j$ |
| $\tilde{s}_i = \sum_{j\neq i}\tilde{w}_{ij} = \frac{s_i}{w_{tot}}$ | $\langle \tilde{s}_i\rangle = \tilde{s}_i$ |
| $k_i = \sum_{j\neq i} a_{ij}$ | $\langle k_i\rangle = \sum_{j\neq i} p_{ij}$ |
| $\tilde{s}_i^{nn} = \frac{\sum_{j\neq i} a_{ij}\tilde{s}_j}{k_i}$ | $\langle \tilde{s}_i^{nn}\rangle = \frac{\sum_{j\neq i} p_{ij}\tilde{s}_j}{\langle k_i\rangle}$ |
| $\tilde{c}_i = \frac{\sum_{j\neq i}\sum_{k\neq i,j}\tilde{w}_{ij}^{1/3}\tilde{w}_{jk}^{1/3}\tilde{w}_{ki}^{1/3}}{\sum_{j\neq i}\sum_{k\neq i,j} a_{ij}a_{ik}}$ | $\langle \tilde{c}_i\rangle = \frac{\sum_{j\neq i}\sum_{k\neq i,j}\langle\tilde{w}_{ij}^{1/3}\rangle\langle\tilde{w}_{jk}^{1/3}\rangle\langle\tilde{w}_{ki}^{1/3}\rangle}{\sum_{j\neq i}\sum_{k\neq i,j} p_{ij}p_{ik}}$ |
| $P_<(w)$ | $\langle P_<(w)\rangle = 1 - \frac{\sum_i\sum_{j<i} p_{ij}^w}{N(N-1)/2}$ |
| $P_<^+(w)$ | $\langle P_<^+(w)\rangle = 1 - \frac{\sum_i\sum_{j<i} p_{ij}^w}{\sum_i\sum_{j<i} p_{ij}}$ |
| **Empirical directed properties** | **Expected directed properties** |
| $w_{ij}$ | $\langle w_{ij}\rangle = \frac{x_i y_j}{1-x_i y_j}$ |
| $\tilde{w}_{ij} = \frac{w_{ij}}{w_{tot}}$ | $\langle \tilde{w}_{ij}\rangle = \frac{\langle w_{ij}\rangle}{\langle w_{tot}\rangle} = \frac{\langle w_{ij}\rangle}{w_{tot}}$ |
| $a_{ij} = \Theta(w_{ij})$ | $\langle a_{ij}\rangle = p_{ij} = x_i y_j$ |
| $\tilde{s}_i^{in} = \sum_{j\neq i}\tilde{w}_{ji} = \frac{s_i^{in}}{w_{tot}}$ | $\langle \tilde{s}_i^{in}\rangle = \tilde{s}_i^{in}$ |
| $\tilde{s}_i^{out} = \sum_{j\neq i}\tilde{w}_{ij} = \frac{s_i^{out}}{w_{tot}}$ | $\langle \tilde{s}_i^{out}\rangle = \tilde{s}_i^{out}$ |
| $\tilde{s}_i^{tot} = \tilde{s}_i^{in} + \tilde{s}_i^{out}$ | $\langle \tilde{s}_i^{tot}\rangle = \langle\tilde{s}_i^{in}\rangle + \langle\tilde{s}_i^{out}\rangle = \tilde{s}_i^{tot}$ |
| $k_i^{in} = \sum_{j\neq i} a_{ji}$ | $\langle k_i^{in}\rangle = \sum_{j\neq i} p_{ji}$ |
| $k_i^{out} = \sum_{j\neq i} a_{ij}$ | $\langle k_i^{out}\rangle = \sum_{j\neq i} p_{ij}$ |
| $k_i^{tot} = k_i^{in} + k_i^{out}$ | $\langle k_i^{tot}\rangle = \langle k_i^{in}\rangle + \langle k_i^{out}\rangle = k_i^{tot}$ |
| $k_i^{\leftrightarrow} = \sum_{j\neq i} a_{ij}a_{ji}$ | $\langle k_i^{\leftrightarrow}\rangle = \sum_{j\neq i} p_{ij}p_{ji}$ |
| $\tilde{s}_i^{in/in} = \frac{\sum_{j\neq i} a_{ji}\tilde{s}_j^{in}}{k_i^{in}}$ | $\langle \tilde{s}_i^{in/in}\rangle = \frac{\sum_{j\neq i} p_{ji}\tilde{s}_j^{in}}{\langle k_i^{in}\rangle}$ |
| $\tilde{s}_i^{in/out} = \frac{\sum_{j\neq i} a_{ji}\tilde{s}_j^{out}}{k_i^{in}}$ | $\langle \tilde{s}_i^{in/out}\rangle = \frac{\sum_{j\neq i} p_{ji}\tilde{s}_j^{out}}{\langle k_i^{in}\rangle}$ |
| $\tilde{s}_i^{out/in} = \frac{\sum_{j\neq i} a_{ij}\tilde{s}_j^{in}}{k_i^{out}}$ | $\langle \tilde{s}_i^{out/in}\rangle = \frac{\sum_{j\neq i} p_{ij}\tilde{s}_j^{in}}{\langle k_i^{out}\rangle}$ |
| $\tilde{s}_i^{out/out} = \frac{\sum_{j\neq i} a_{ij}\tilde{s}_j^{out}}{k_i^{out}}$ | $\langle \tilde{s}_i^{out/out}\rangle = \frac{\sum_{j\neq i} p_{ij}\tilde{s}_j^{out}}{\langle k_i^{out}\rangle}$ |
| $\tilde{s}_i^{tot/tot} = \frac{\sum_{j\neq i}(a_{ij}+a_{ji})\tilde{s}_j^{tot}}{k_i^{tot}}$ | $\langle \tilde{s}_i^{tot/tot}\rangle = \frac{\sum_{j\neq i}(p_{ij}+p_{ji})\tilde{s}_j^{tot}}{\langle k_i^{tot}\rangle}$ |
| $\tilde{c}_i^{in} = \frac{\sum_{j\neq i}\sum_{k\neq i,j}\tilde{w}_{jk}^{1/3}\tilde{w}_{ji}^{1/3}\tilde{w}_{ki}^{1/3}}{k_i^{in}(k_i^{in}-1)}$ | $\langle \tilde{c}_i^{in}\rangle = \frac{\sum_{j\neq i}\sum_{k\neq i,j}\langle\tilde{w}_{jk}^{1/3}\rangle\langle\tilde{w}_{ji}^{1/3}\rangle\langle\tilde{w}_{ki}^{1/3}\rangle}{\sum_{j\neq i}\sum_{k\neq i,j} p_{ji}p_{ki}}$ |
| $\tilde{c}_i^{out} = \frac{\sum_{j\neq i}\sum_{k\neq i,j}\tilde{w}_{ik}^{1/3}\tilde{w}_{ij}^{1/3}\tilde{w}_{jk}^{1/3}}{k_i^{out}(k_i^{out}-1)}$ | $\langle \tilde{c}_i^{out}\rangle = \frac{\sum_{j\neq i}\sum_{k\neq i,j}\langle\tilde{w}_{ik}^{1/3}\rangle\langle\tilde{w}_{ij}^{1/3}\rangle\langle\tilde{w}_{jk}^{1/3}\rangle}{\sum_{j\neq i}\sum_{k\neq i,j} p_{ij}p_{ik}}$ |
| $\tilde{c}_i^{cyc} = \frac{\sum_{j\neq i}\sum_{k\neq i,j}\tilde{w}_{ij}^{1/3}\tilde{w}_{jk}^{1/3}\tilde{w}_{ki}^{1/3}}{k_i^{in}k_i^{out}-k_i^{\leftrightarrow}}$ | $\langle \tilde{c}_i^{cyc}\rangle = \frac{\sum_{j\neq i}\sum_{k\neq i,j}\langle\tilde{w}_{ij}^{1/3}\rangle\langle\tilde{w}_{jk}^{1/3}\rangle\langle\tilde{w}_{ki}^{1/3}\rangle}{\langle k_i^{in}\rangle\langle k_i^{out}\rangle-\sum_{j\neq i} p_{ij}p_{ji}}$ |
| $\tilde{c}_i^{mid} = \frac{\sum_{j\neq i}\sum_{k\neq i,j}\tilde{w}_{ik}^{1/3}\tilde{w}_{jk}^{1/3}\tilde{w}_{ji}^{1/3}}{k_i^{in}k_i^{out}-k_i^{\leftrightarrow}}$ | $\langle \tilde{c}_i^{mid}\rangle = \frac{\sum_{j\neq i}\sum_{k\neq i,j}\langle\tilde{w}_{ik}^{1/3}\rangle\langle\tilde{w}_{jk}^{1/3}\rangle\langle\tilde{w}_{ji}^{1/3}\rangle}{k_i^{in}k_i^{out}-\sum_{j\neq i} p_{ij}p_{ji}}$ |
| $\tilde{c}_i^{tot} = \frac{\sum_{j\neq i}\sum_{k\neq i,j}(\tilde{w}_{ij}^{1/3}+\tilde{w}_{ji}^{1/3})(\tilde{w}_{jk}^{1/3}+\tilde{w}_{kj}^{1/3})(\tilde{w}_{ki}^{1/3}+\tilde{w}_{ik}^{1/3})}{2\left[k_i^{tot}(k_i^{tot}-1)-2k_i^{\leftrightarrow}\right]}$ | $\langle \tilde{c}_i^{tot}\rangle = \frac{\sum_{j\neq i}\sum_{k\neq i,j}\langle\tilde{w}_{ij}^{1/3}+\tilde{w}_{ji}^{1/3}\rangle\langle\tilde{w}_{jk}^{1/3}+\tilde{w}_{kj}^{1/3}\rangle\langle\tilde{w}_{ki}^{1/3}+\tilde{w}_{ik}^{1/3}\rangle}{2\left[\sum_{j\neq i}\sum_{k\neq i,j}(p_{ji}p_{ki}+p_{ij}p_{ik})+2(k_i^{in}k_i^{out})-2\sum_{j\neq i} p_{ij}p_{ji}\right]}$ |
| $P_<(w)$ | $\langle P_<(w)\rangle = 1 - \frac{\sum_i\sum_{j\neq i} p_{ij}^w}{N(N-1)/2}$ |
| $P_<^+(w)$ | $\langle P_<^+(w)\rangle = 1 - \frac{\sum_i\sum_{j\neq i} p_{ij}^w}{\sum_i\sum_{j\neq i} p_{ij}}$ |

TABLE I: Expressions for the empirical and expected properties in the weighted (undirected and directed) representations of the network.

vertex $j$ is derived from the weight matrix by setting $a_{ij} = \Theta(w_{ij})$, where $\Theta(x) = 1$ if $x > 0$ and $\Theta(x) = 0$ otherwise. The probability that vertices $i$ and $j$ are connected, irrespective of the edge weight, is now $\langle a_{ij}\rangle = p_{ij} \equiv 1 - q_{ij}(0) = x_i x_j$. In analogy with the expectation values of products of weights, we have $\langle a_{ij}a_{kl}\rangle = p_{ij}p_{kl}$ if $(i-j)$ and $(k-l)$ are distinct pairs of vertices, whereas $\langle a_{ij}a_{kl}\rangle = \langle a_{ij}^2\rangle = \langle a_{ij}\rangle = p_{ij}$ if $(i-j)$ and $(k-l)$ are the same pair of vertices. Finally note that we are interested in studying the quantities obtained using the rescaled weights $\tilde{w}_{ij} = w_{ij}/w_{tot}$. This does not introduce complications, since $\langle w_{tot}\rangle = w_{tot}$ as we have shown in Eq. (2). However, the parameters $\{x_i\}$ are computed as in Eq. (A4) before rescaling the strengths, since the original integer weights $w_{ij}$ are the actual degrees of freedom.

## APPENDIX B: WEIGHTED DIRECTED PROPERTIES

In the weighted directed case, the above results can be generalized as follows. Each graph $\mathbf{G}$ is completely specified by its non-negative (integer-valued) weight matrix $\mathbf{W}$, which now is in general not symmetric. The constraints specified in the randomization method [2] are now the joint in-strength and out-strength sequence: $\{C_a\} = \{s_i^{in}, s_i^{out}\}$. The Hamiltonian takes the form

$$H(\mathbf{W}) = \sum_i \left[\theta_i^{in} s_i^{in}(\mathbf{W}) + \theta_i^{out} s_i^{out}(\mathbf{W})\right] \tag{B1}$$

The above choice leads to the graph probability [2]

$$P(\mathbf{W}) = \prod_i \prod_{j\neq i} q_{ij}(w_{ij}) \tag{B2}$$

where

$$q_{ij}(w) = (x_i y_j)^w (1 - x_i y_j) \tag{B3}$$

(with $x_i \equiv e^{-\theta_i^{out}}$ and $y_i \equiv e^{-\theta_i^{in}}$) is the probability that a link of weight $w$ exists from vertex $i$ to vertex $j$ in the maximum-entropy ensemble of weighted directed graphs with specified in- and out-strength sequences. If the empirical strength sequences $\{s_i^{in}(\mathbf{W}^*)\}$ and $\{s_i^{out}(\mathbf{W}^*)\}$ of a particular real directed weighted network $\mathbf{W}^*$ are chosen as constraints, then Eq. (B3) yields the exact value of the connection probability in the ensemble of randomized directed weighted graphs with the same average strength sequences as the empirical ones, provided that the parameters $\{x_i\}$ and $\{y_i\}$ are set to the values that maximize the likelihood $P(\mathbf{W}^*)$ [2]. These values are the solution of the following set of $2N$ coupled non-linear equations [10]:

$$\langle s_i^{out}\rangle = \sum_{j\neq i} \frac{x_i y_j}{1 - x_i y_j} = s_i^{out}(\mathbf{W}^*) \quad \forall i \tag{B4}$$

$$\langle s_i^{in}\rangle = \sum_{j\neq i} \frac{x_j y_i}{1 - x_j y_i} = s_i^{in}(\mathbf{W}^*) \quad \forall i \tag{B5}$$

After the values $\{x_i\}$ and $\{y_i\}$ are found and plugged into Eq. (B3), the expectation value $\langle X\rangle$ of any topological property $X$ can be calculated analytically, avoiding the numerical generation of the random ensemble [2]. Now, by construction, the in-strengths and out-strengths of all vertices are special local quantities whose expected and empirical values are exactly equal: $\langle s_i^{in}\rangle = s_i^{in}$ and $\langle s_i^{out}\rangle = s_i^{out}$ as shown in Eq. (B5). The higher-order topological properties considered in the main text have the expectation values shown in Table I, obtained using the same prescriptions as in the undirected case, with two differences. The first one is that now

$$\langle w_{ij}^{\alpha}\rangle \equiv \sum_w w^{\alpha} q_{ij}(w) = (1 - x_i y_j)\mathrm{Li}_{-\alpha}(x_i y_j) \tag{B6}$$

where $\mathrm{Li}_n(z)$ is still the Polylogarithm function defined in Eq. (A6). Thus $\langle w_{ij}\rangle = x_i y_j/(1 - x_i y_j)$ and $\langle a_{ij}\rangle = p_{ij} \equiv 1 - q_{ij}(0) = x_i y_j$, where $a_{ij} = \Theta(w_{ij})$. The expectation values of other powers of the weight change accordingly. The second one is that, as in the binary directed case, $(i - j)$ and $(j - i)$ are different (and statistically independent) directed pairs of vertices. Therefore $\langle w_{ij} w_{ji}\rangle = \langle w_{ij}\rangle\langle w_{ji}\rangle$ and $\langle a_{ij} a_{ji}\rangle = p_{ij} p_{ji}$. Again, we have $\langle w_{tot}\rangle = w_{tot}$ as we have shown in Eq. (8). Therefore we can still easily obtain the quantities built on the rescaled weights $\tilde{w}_{ij} = w_{ij}/w_{tot}$. As for the weighted undirected case, the parameters $\{x_i\}$ and $\{y_i\}$ are however computed using Eq. (B5) before rescaling the strengths, preserving the original integer weights $w_{ij}$ as the actual degrees of freedom.


[1] T. Squartini, G. Fagiolo, and D. Garlaschelli, LEM WP Series 2011–08, Laboratory of Economics and Management (LEM) (2011).

[2] T. Squartini and D. Garlaschelli, Preprint arXiv:1103.0701v1 [physics.data-an] (2011).

[3] J. Saramäki, M. Kivelä, J.-P. Onnela, K. Kaski, and J. Kertész, Physical Review E **75**, 027105 (2007).

[4] G. Fagiolo, Physical Review E **76**, 026107 (2007).

[5] R. Feenstra, *Advanced international trade : theory and evidence* (Princeton University Press, 2004).

[6] P. van Bergeijk and S. Brakman, eds., *The Gravity Model in International Trade* (Cambridge University Press, Cambridge, 2010).

[7] G. Fagiolo, Journal of Economic Interaction and Coordination **5**, 1 (2010).

[8] K. Bhattacharya, G. Mukherjee, J. Sarämaki, K. Kaski, and S. Manna, Journal of Statistical Mechanics: Theory Exp. A **2**, P02002 (2008).

[9] D. Garlaschelli and M. I. Loffredo, Physical Review Letters **102**, 038701 (2009).

[10] D. Garlaschelli and M. I. Loffredo, Physical Review E **78**, 015101 (2008).